PROCEEDINGS OF SPIE

SPIEDigitalLibrary.org/conference-proceedings-of-spie

Modeling the effects of bipolar helical cuff electrodes in vagus nerve stimulation

Ding, Alice, Luo, Ma, Miga, Michael

Alice K. Ding, Ma Luo, Michael I. Miga, "Modeling the effects of bipolar helical cuff electrodes in vagus nerve stimulation," Proc. SPIE 11598, Medical Imaging 2021: Image-Guided Procedures, Robotic Interventions, and Modeling, 115982H (15 February 2021); doi: 10.1117/12.2582182

SPIE.

Event: SPIE Medical Imaging, 2021, Online Only

Modeling the Effects of Bipolar Helical Cuff Electrodes in Vagus Nerve Stimulation

Alice K. Ding[1,2,3], Ma Luo[1,3], Michael I. Miga[1,3,4,5,6]
[1]Vanderbilt Institute for Surgery and Engineering, Nashville, TN USA
[2]SyBBURE Searle Undergraduate Research Program, Nashville, TN USA
[3]Vanderbilt University, Department of Biomedical Engineering, Nashville, TN USA
[4]Vanderbilt University Medical Center, Department of Radiology and Radiological Sciences, Nashville, TN USA
[5]Vanderbilt University Medical Center, Department of Neurological Surgery, Nashville, TN USA
[6]Vanderbilt University Medical Center, Department of Otolaryngology – Head and Neck Surgery, Nashville, TN USA

Keywords: Vagus nerve stimulation, finite element modeling, bipolar helical cuff, neural computational modeling, epilepsy

ABSTRACT

While mainly used for reducing seizures in epileptic patients, vagus nerve stimulation (VNS) has been implied to be capable of treating various other diseases. However, the therapeutic extent and control of neuromodulation for these conditions are still uncertain and are limited by the ability to predict neural activation responses upon targeting certain fascicles. Generally, VNS is administered through a bipolar helical cuff electrode implanted around the left vagus nerve. The electrode delivers pulses of electricity to the nerve to recruit axons. This work focuses on predicting percent activation and regions of activation based on different adjustable factors such as injected current amplitude and pulse width of stimuli and the activated region of the electrode. To achieve, a simplified finite element model was created using cylindrical geometries as nerve components with an addition of helical cuff electrodes. All of these components were encased in surrounding tissue with assumed properties similar to adipose. Electric potential distribution in the model was processed with an activating function defined along the axonal length which estimates the injected current at the nodes of Ranvier (NoR). These values were then enforced in the neuron simulation as a current clamp approximation applied at the NoR and the likelihood of an action potential was determined. Presence of action potentials were then detected to determine which axons were recruited in VNS. This preliminary work determined that electrode configurations can target specific fascicles in the nerve while amplitudes and pulse widths of stimuli contribute to the percentage of the nerve activated. This demonstrates the ability for patient-specific control over targeting fascicles. Additionally, this work presents initial steps to improving the model by using histological data to create a geometric-specific approach.

1 INTRODUCTION

Vagus nerve stimulation (VNS) has been mostly performed to treat drug-resistant patients with epilepsy or depression since FDA approval in the last two decades [1, 2]. However, initial studies and reports have indicated that this treatment could also be used to treat obesity, bipolar, Alzheimer's, heart failure and more [2]. As a surgical intervention approach, VNS leverages electric stimulation of the nervous system via an implantable device. Specifically, VNS is administered through a bipolar helical cuff electrode with adjustable parameters such as frequency, pulse width, amplitude and activated regions of the electrodes. The electrode delivers pulses of electric stimulation to the nerve fibers creating an inhibitive bioelectric effect arresting or dampening the seizure in the case of epilepsy. Certain axons instigate different effects in the patient, such as reducing seizures.

Undesirable symptoms of left VNS treatment include voice alteration, cough, dyspnea, dysphagia, and neck pain [2]. These are often caused by off-target stimulation of certain fascicles or exceeding the amount of activation needed. The effectiveness of VNS is dependent on optimizing stimulation parameters and accurately targeting fascicles [3]. To better individualize the treatment, computational modeling can be used to predict regions of activation (ROA) in the vagus nerve and predict its effects when certain fascicles are activated. Already, effects of VNS have been linked to certain fibers in

Medical Imaging 2021: Image-Guided Procedures, Robotic Interventions, and Modeling,
edited by Cristian A. Linte, Jeffrey H. Siewerdsen, Proc. of SPIE Vol. 11598, 115982H

the nerve through neuroanatomical tracing techniques [4]. Prior literature presents methods to improving nerve models and investigating what effects certain modeling approaches can have on the accuracy of predicting VNS therapy [5].

While fiber activation can be estimated based on scaling the activation from that of a feline preclinical animal model such as in [6], the work presented here demonstrates a method using NEURON 5.7 to find NoR, and therefore axons, that generate an action potential from a certain injected current stimulus [7]. In this work, injected current amplitudes, pulse widths, and electrode configurations were all investigated to determine their effects on ROA and percent activation. The objective of this study is present a method that predicts the location and extent the nerve is activated given different settings and configurations of the electrode.

2 METHODS

2.1 Finite Element Models of Nerves and Electrodes

A finite element model (FEM) of a simplified nerve was implemented in COMSOL Multiphysics® (COMSOL AB, Stockholm, Sweden) in which geometries were limited to cylindrical shapes [8]. The nerve contained four fascicles: one in the center, one near the center of the electrode, one near the circumferential end of the electrode, and the final one in a region not covered by the electrode. The helical electrodes were designed to only wrap around 3/4th of the nerve. This was all encompassed by a domain representing the region outside of the nerve (carotid space) which was designated to have properties similar to adipose (**Figure 1a**). Both the nerve's and the cuff electrodes' geometric and electrical properties are outlined in detail in **Table 1** [5, 6, 9 - 12]. A tetrahedral finite element mesh was generated with refinement; it consisted of 2,834,073 elements and 474,464 nodes (**Figure 1b**).

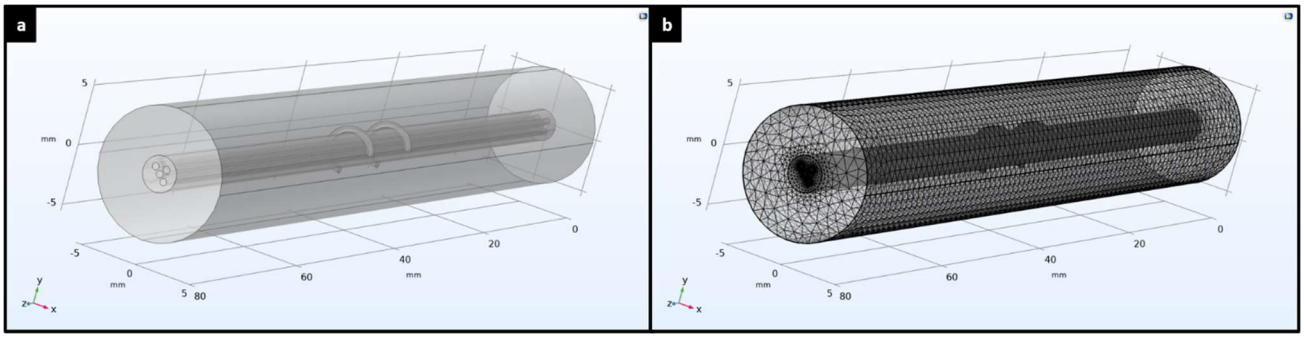

Figure 1. (a) Geometric representation of the nerve model with helical electrodes which encompasses 270° of the nerve. **(b)** Tetrahedral finite element mesh of the nerve and cuff electrode model.

Table 1. The geometric and electrical properties of the components in the nerve model and the cuff electrodes.

	Geometric and Electrical Properties of the Nerve				
	Height *(mm)*	Diameter *(mm)*	Offset *(mm)*	Conductivity *(S/m)*	Relative Permittivity
Epineurium	80	3	N/A	0.1587	21600
Endoneurium	80	0.6	(0.5, 0.5), (-0.5, 0.5), (0.5, -0.5), (0, 0)	(0.08, 0.08, 0.57)	21600
Adipose Tissue	80	11	N/A	0.0432	393
	Geometric and Electrical Properties of the Helical Cuff Electrodes				
	Number of turns	Minor Radius *(mm)*	Gap between Electrodes *(mm)*	Conductivity *(S/m)*	Relative Permittivity
Platinum Iridium	0.75	0.4	8	107	1

The boundary conditions used in this study followed [6]. The lateral boundary of the region, highlighted in blue in **Figure 2a** representing tissue surrounding the nerve was set to ground. More specifically, the backside of the electrode (boundaries not touching the nerve) and the ends of the nerve were set to be electrically insulated as shown in blue in **Figure 2b**. The electrodes, applied to the boundaries touching the nerve as shown in **Figure 2c**, were given an injected current stimulus

incrementally from 0.75 to 3.5 mA, the maximum tolerable current amplitude used in VNS [12]. The electric potential distribution was generated under these conditions in a stationary study.

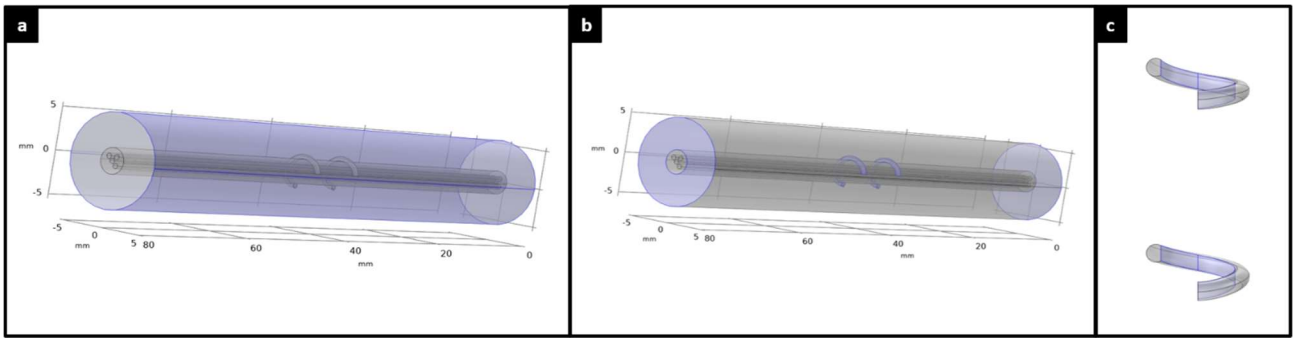

Figure 2. (a) Boundaries set to ground (blue) in the nerve model. **(b)** Boundaries set to electrical insulation (blue) in the nerve model. **(c)** Boundaries (blue) where the injected current stimulus is applied to the helical electrodes.

2.2 Modeling Regions of Activation

The electric potentials were then interpolated onto a grid in accordance to the geometric shape of the nerve with spacing of 0.1 mm between points in the cross-sectional direction. In the direction traveling down the nerve, the grid spacing was defined by the spacing between the NoR. Between the NoR, the spacing is dependent on the diameter of the axons, e.g., for 5.7 µm, it is 0.5 mm [13]. Afterwards, the points that did not lie in fascicles were then removed (**Figure 3a**). Along each axon, the follow equation that represents an activation function was used [14]:

$$f = \frac{d}{4p_i c} \times \frac{d^2 V^e}{dx^2}$$

where f is the current clamp input (A), p_i is axoplasmic resistivity (Ω cm), c is capacitance of the NoR (µF/cm^2), d is the diameter of the axon fiber (µm), V^e is extracellular voltage (V), and x is position along the axon (mm).

For this study, the properties were used: axoplasmic resistivity was 70 Ω cm, capacitance was 2 µF/cm^2, and the diameter of each axon fiber was 5.7 µm [13]. This allowed for the current clamp input along an axon at each node to be determined using the second derivative of the extracellular voltages (**Figure 3b**). Subsequently, at each of these NoR, whether an action potential occurred given its input was found using NEURON 5.7 [7]. To achieve, an axon was built linearly along the nerve at a length of 80 mm and divided into as many sections as there are NoR. The input at each NoR was then applied to the axon as a current clamp with a pulse width of 500 µs. Axons were considered activated if any of the NoR along that axon generated an action potential. This study applied this method to examining the effects of injected current amplitudes, pulse widths, and electrode configurations. Additionally, to understand the limitations of this study, axon diameters were also analyzed.

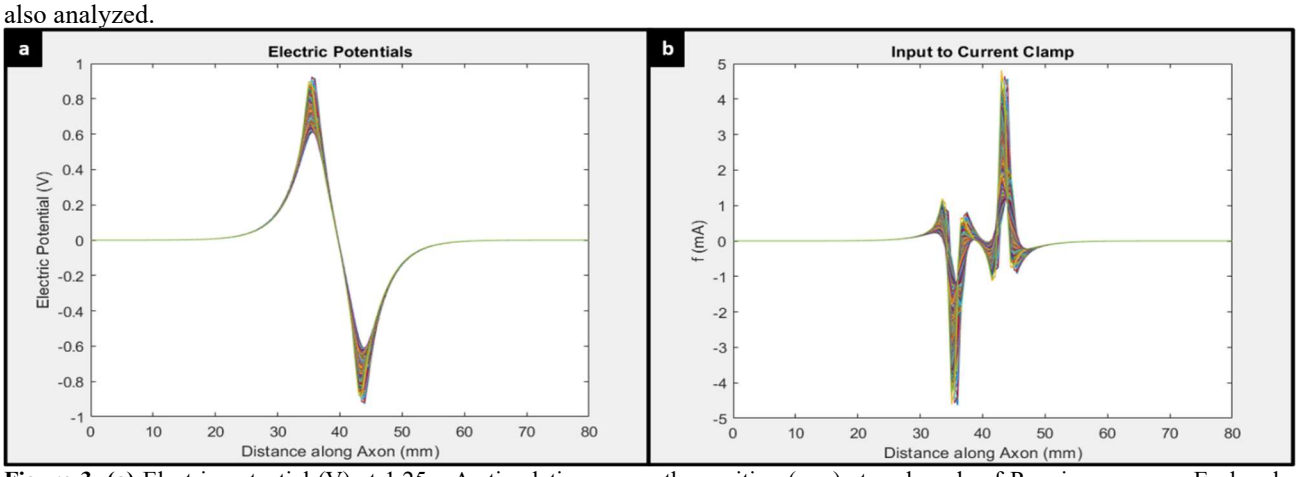

Figure 3. (a) Electric potential (V) at 1.25 mA stimulation versus the position (mm) at each node of Ranvier per axon. Each color represents an axon in the fascicles. **(b)** Current clamp input (mA) compared to the position (mm) of NoR along an axon. Each color represents an axon in the fascicles.

3 RESULTS

3.1 Effect of Current Stimulation Amplitudes and Pulse Widths on Regions of Activation

Since the therapeutic current stimulus used in VNS is normally in the amplitude range of 1.0 - 1.5 mA, electric potentials were found for injected current amplitudes in the range 0.75 – 2.0 mA (**Figure 4**).

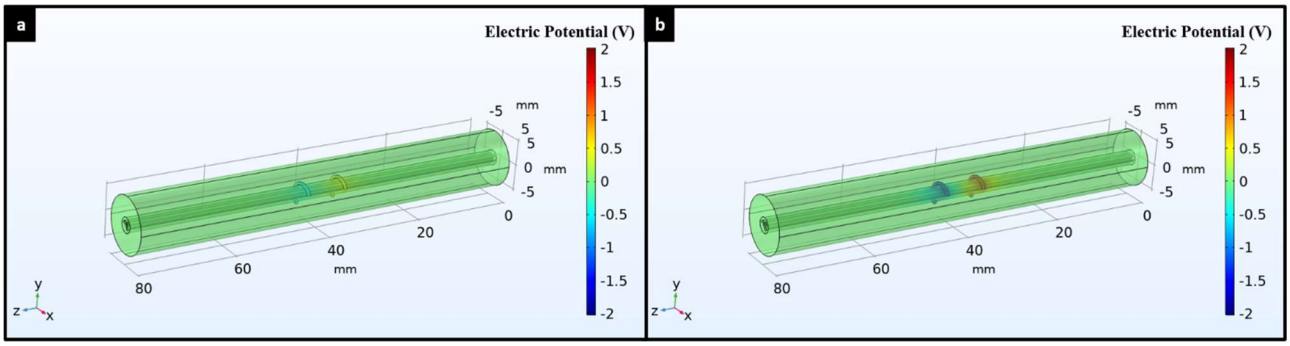

Figure 4. Electric potential (V) distributions of the simplified nerve model for **(a)** 0.75 mA and **(b)** 2.0 mA amplitude stimulus on the electrodes.

Consequently, the ROA was also found (**Figure 5**). As expected, the number of axons activated increased as evident by the regions in red as the injected current is increased. It was determined that the fascicles in closer proximity to the electrode needed smaller magnitude stimulus current as opposed to those further away.

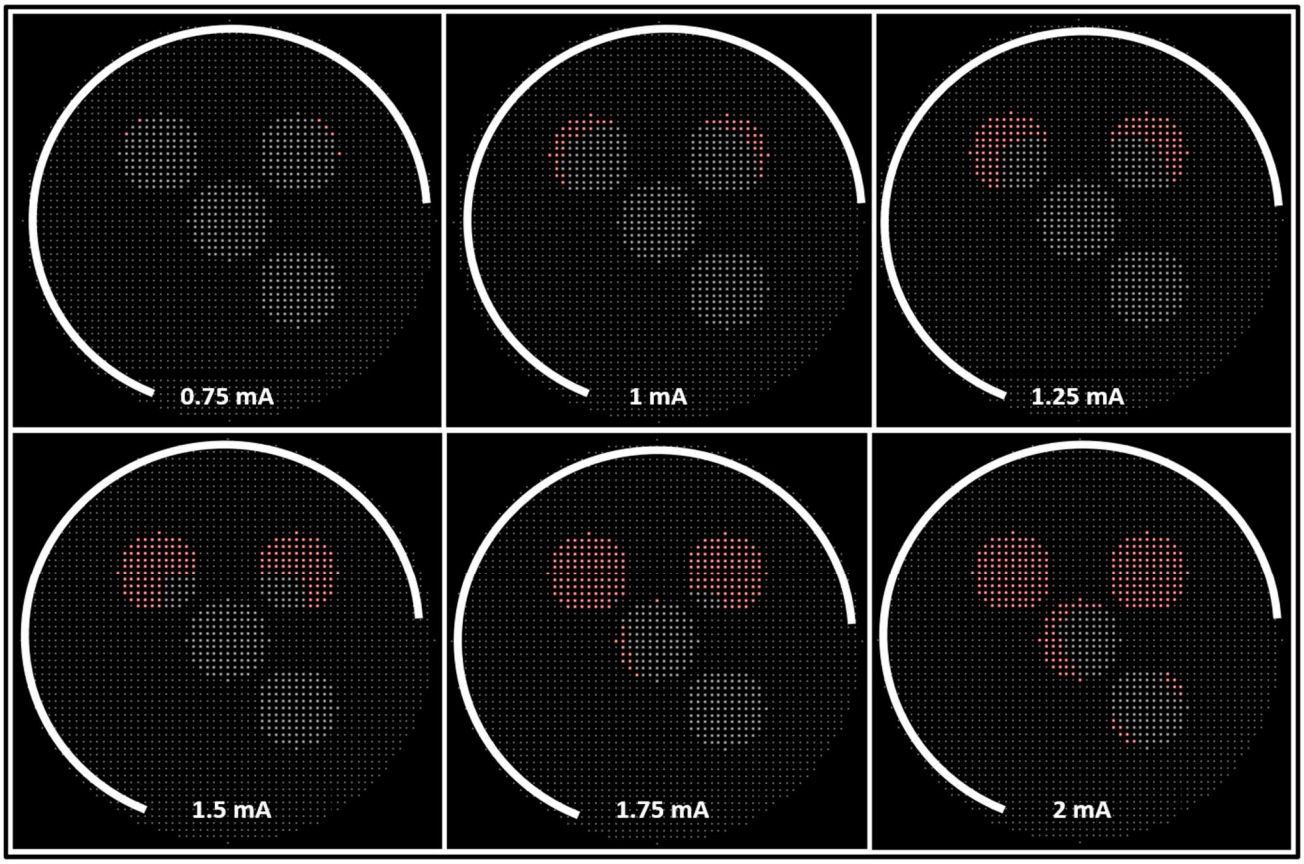

Figure 5. ROA (red) for injected current amplitudes stimulating the electrode from 0.75 to 2.0 mA. The fascicles not activated (white) decrease with greater stimulus by the electrode (white solid circle).

The results demonstrated earlier used 500 μs pulse widths. To investigate effects pulse widths have on neural activation, 250 μs was also examined as this is also a pulse width frequently used in treating epilepsy [12]. The percent of nerve activation was found and compared between the two different pulse widths to understand the level of influence over activation this parameter offers as shown in **Figure 6**.

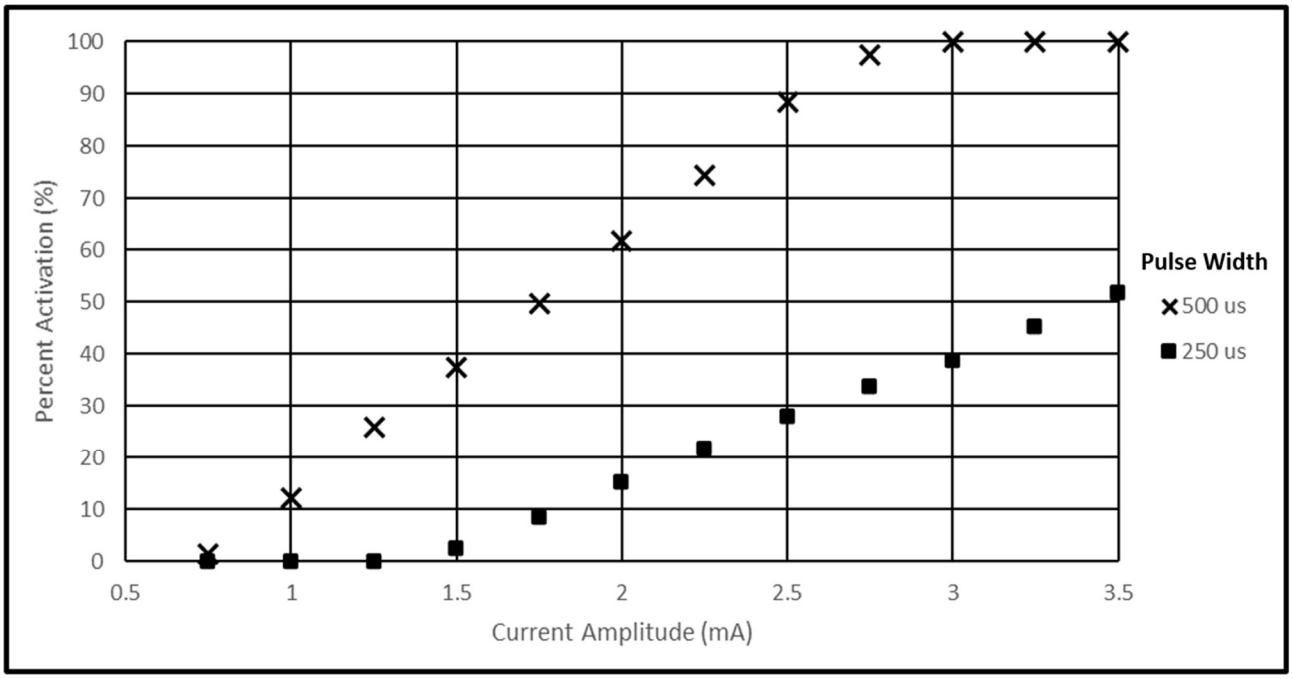

Figure 6. The percent activation for injected current amplitudes the electrode is stimulated with compared between 250 and 500 μs pulse width.

3.2 Effect of Electrode Configurations on Neural Activation

The electrodes were divided into three different sections and activated one at a time to see how that would affect ROA (recall that the electrode encompasses ¾ of the nerve). In each of the electrodes, a third of the boundary was activated to see if the fascicle closest to it could be targeted. When the stimulus initially tested was 2.0 mA, the two fascicles nearest to the electrode were activated (**Figure 7**). When the bottom was activated, the edges of fascicles closest to it were only slightly activated because there is no direct fascicle. After the amplitude was lowered to 1.25 mA, only one fascicle and the edge of another near fascicle is activated showing that a particular fascicle, if chosen the correct electrode configuration and amplitude, can be targeted. Please note the impact of the configurations on activation coverage is a gradient dependent on the distance between the electrodes and the axons.

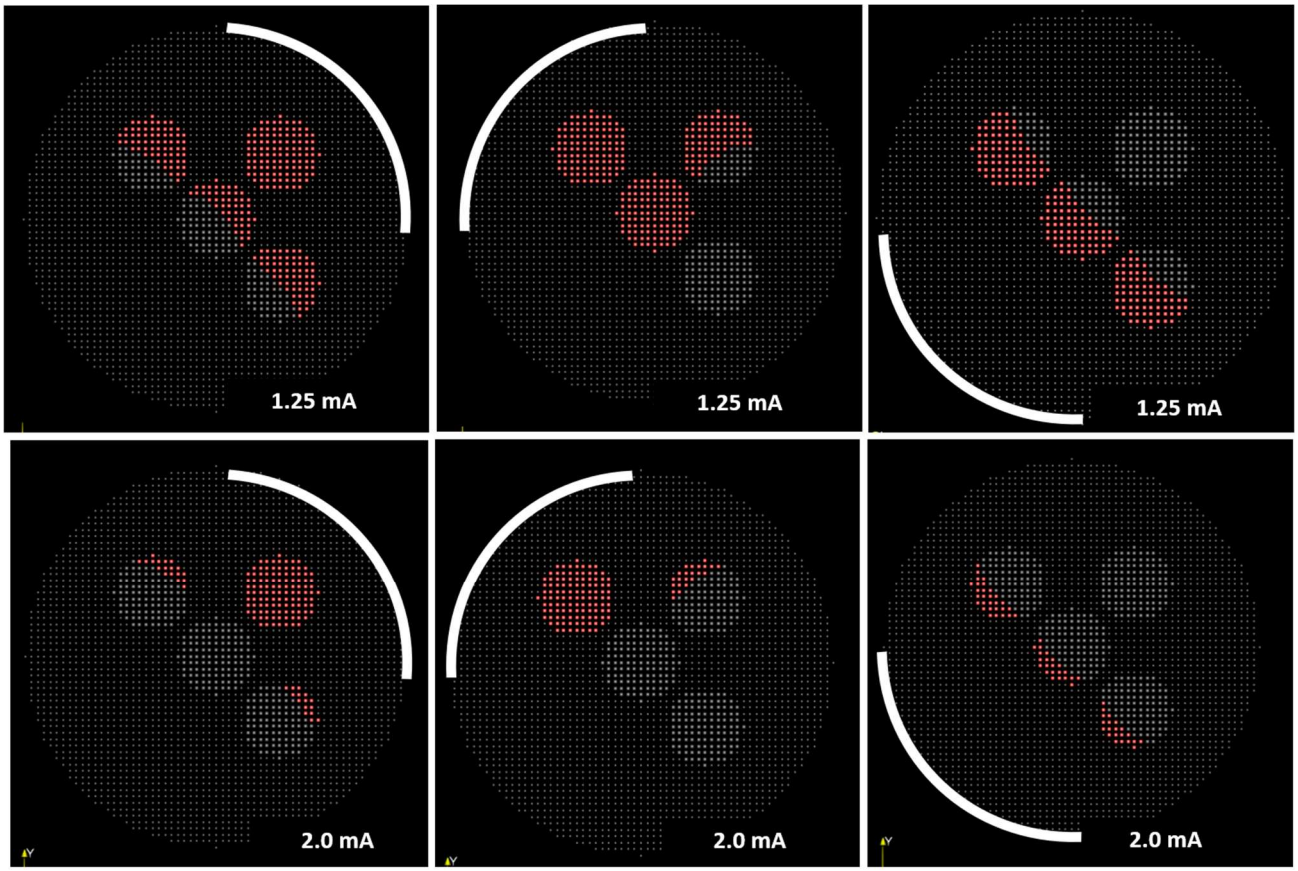

Figure 7. ROA (red) when 1.25 mA or 2.0 mA are given as a stimulus with different electrode configurations (solid white).

3.3 Incorporating Histological Data

To improve specificity, a stained histological photograph from [2] was used to create a more accurate nerve geometric shape with a more realistic distribution of fascicles. It was then scaled to have a diameter similar to the human vagus nerve, ~6.5 mm [15]. The electrode was scaled up to fit the modified nerve model as well. To complete the computational domain, the encompassing region around the model had a diameter of 14.5 mm. For both the nerve and electrodes, the electrical properties remained the same as the simplified nerve model (**Figure 8a**). A tetrahedral mesh was generated with a total of 3,365,739 elements and 563,178 nodes (**Figure 8b**)

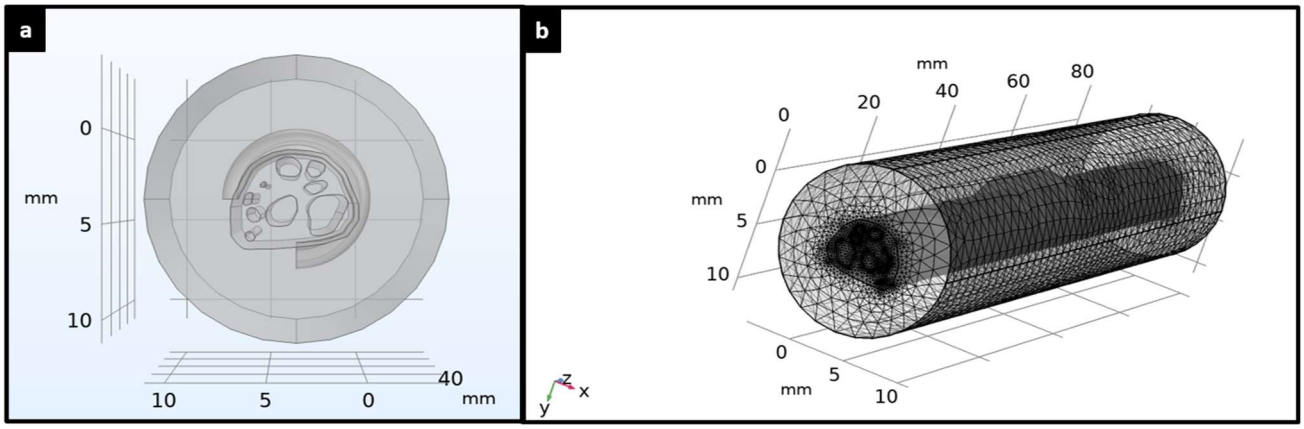

Figure 8. (a) Geometric model of the nerve and electrodes using the stained histological photograph as a cross-sectional base. **(b)** The tetrahedral mesh generated from the geometric model.

Electric potentials were calculated for the model at the maximum tolerable level in VNS, 3.5 mA (**Figure 9a**), using the same boundary conditions as described above [12]. This was chosen because the diameter of the nerve was scaled to be on the larger end of vagus nerves. The ROA for each fascicle in the new nerve model was shown highlighted in red in **Figure 9b**.

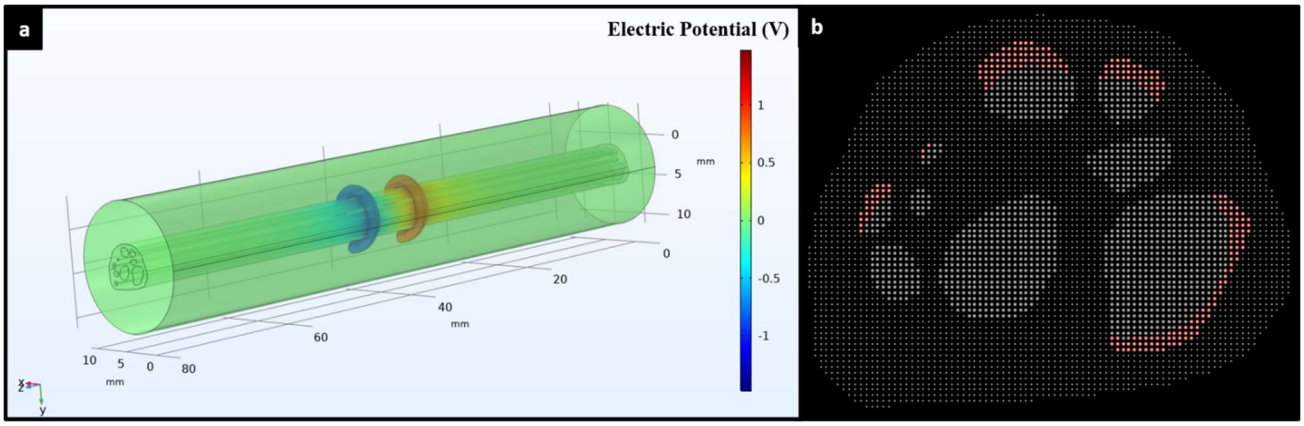

Figure 9. (a) The electric potential distribution (V) was calculated for the tetrahedral mesh of the histological model. **(b)** The ROA of the new model using 3.5 mA as stimulus.

Additionally, the vagus nerve is composed of different axon diameters. In this study, 5.7 µm was used because most axons from the nerve have a diameter of 5 µm or below [6]. To understand the effects axon diameters have on percent nerve activation, 8.7 µm and 11.5 µm were also used for the same amplitude range (**Figure 10**).

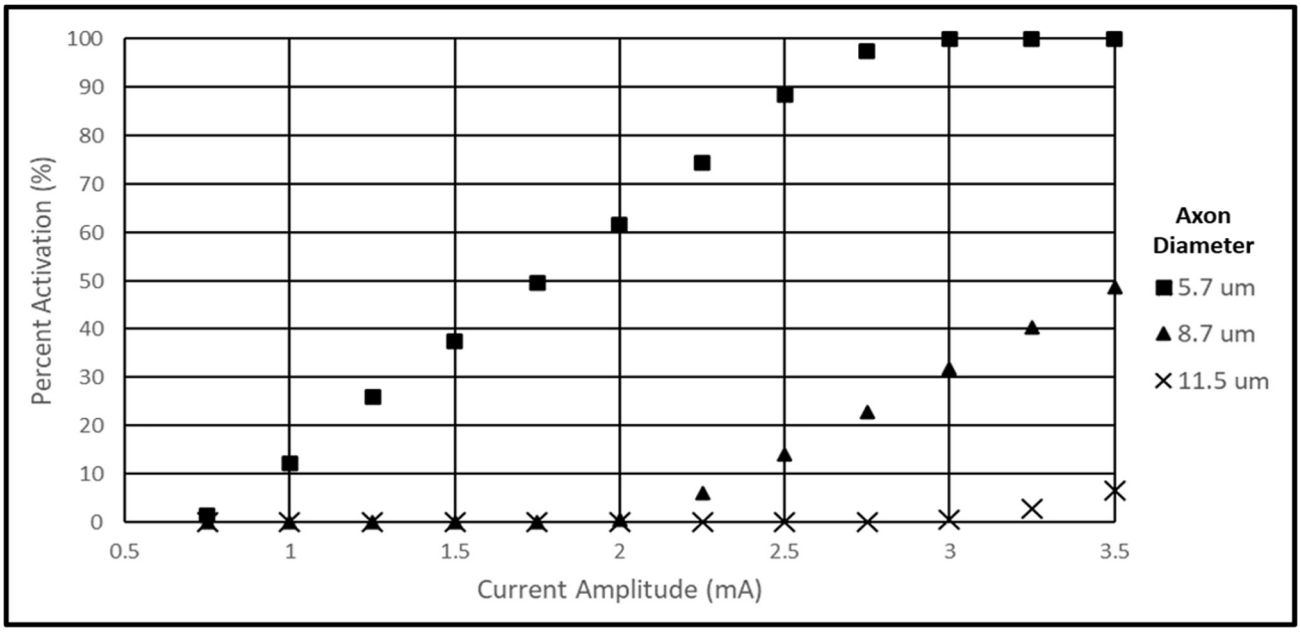

Figure 10. The percent activation for injected current amplitudes the electrode is stimulated with compared between 5.7 µm, 8.7 µm, and 11.5 µm axon diameters.

4 DISCUSSION

The results from this study show how amplitudes and electrode configurations can be adjusted to target recruitment of axons in certain fascicles. The amount of activation and the pattern of activation are indicated by **Figure 5,** showing how amplitudes can manage this particular criterion. Additionally, between 500 µs and 250 µs pulse width, extent of activation

can drastically deviate from each other as shown in **Figure 6**. In **Figure 7**, the ability to target certain fascicles is demonstrated. Overall, the electrode configuration allows for the treatment to have flexibility over the locations in the nerve that are activated while the amplitudes and pulse widths direct the amount of stimulation.

Research has been done to understand the vagus nerve fibers using imaging and tracing of the efferent and afferent fascicles such as its effect on different bodily functions when traced back to certain sections of the brainstem [4]. For example, the dorsal nucleus of the vagus nerve supplies innervation to the heart, lungs, and the gastrointestinal tract, the nucleus ambiguus controls the motor fibers and impacts the heart, the solitary nucleus affects patient's taste, and the spinal trigeminal nucleus affects the patient's ability to detect touch or pain [4]. While more information is needed to be collected about other fascicles, the point remains that it is important for treatment to be able to control the effects on the patient by targeting the correct fascicles. These results show that this is possible to predict using computational modeling which can optimize the correct use of electrode configuration, amplitude, and pulse width.

However, the control over activation is limited due to the properties of the nerve, e.g. nerve and axon diameters. As the cross-sectional diameter of the nerve gets larger, as exemplified by **Figure 9**, more amplitude is needed to activate smaller regions of the nerve. Like the nerve diameter, the amplitude needed to activate the axons are higher for axons with larger diameters as shown in **Figure 10**. This should be accounted for when controlling which fascicles should be activated when determining treatment settings. For future work, more accurate models of vagus nerves could be built using patient specific cross-sectional areas of their nerves as shown by **Figure 9**. This could lead to developing patient-specific models that could enable more customized functional activation for VNS therapies.

5 CONCLUSION

Targeting fascicles to ensure appropriate stimulation is likely critical to reducing side effects and promoting VNS therapy efficacy. Electric potential distributions were calculated for a range of amplitudes using COMSOL Multiphysics® estimated using an activating function to be current clamp approximations. These values were loaded into NEURON as current clamp stimuli. From NEURON, axons where NoR indicated action potentials were recorded for determination of recruitment. The results indicate that electrode configurations could be used to target specific fascicles, while amplitudes could be used to influence the amount of activation occurring. However, variability from patient to patient may lead to reduced efficacy due to geometric differences, electrical properties, and positioning. This causes a need for patient specific models to be developed. In this study, a histological model was created and ROA was able to be found. This model should be improved for future use so that accuracy is increased for predicting its effects.

6 ACKNOWLEDGEMENTS

This work is supported by the National Institutes of Health, the National Institute for Neurological Disorders and Stroke, R01NS049251 and SyBBURE Searle Undergraduate Research Program at Vanderbilt University.

7 REFERENCES

[1] Wu, C., Sharan, A.D., "Neurostimulation for the treatment of epilepsy: a review of current surgical interventions," Neuromodulation 16, 10–24 (2013).
[2] Howland, R.H., "Vagus nerve stimulation," Curr. Behav. Neurosci., 1(2), 64 - 73 (2014).
[3] Ardesch, J.J., et al., "Vagus nerve stimulation for epilepsy activates the vocal folds maximally at therapeutic levels," Epilepsy Res. 89, 227–231 (2010).
[4] Thompson, N., Mastitskaya, S., Holder, D., "Avoiding off-target effects in electrical stimulation of the cervical vagus nerve: neuroanatomical tracing techniques to study fascicular anatomy of the vagus nerve," Journal of Neuroscience Methods 325 (2019).
[5] Pelot, N.A., Behrend, C. E., Grill, W. M., "On the parameters used in finite element modeling of compound peripheral nerves," Journal of Neural Engineering 16(1) (2019).
[6] Arle, J.E., Carlson, K. W., Mei, L., "Investigation of mechanisms of vagus nerve stimulation for seizure using finite element modeling," Epilepsy Research 126, 109-118 (2016).
[7] Hines, M. L., Carnevale, N. T., "NEURON: a tool for neuroscientists," The Neuroscientist 7, 123-135 (2001).
[8] COMSOL Multiphysics® v. 5.4. www.comsol.com. COMSOL AB, Stockholm, Sweden.

[9] Ranck, J. B., Bement, S.L., “The specific impedance of the dorsal columns of cat: an anisotropic medium,” Experimental Neurology 11, 451-463 (1965).
[10] Grill, W. M., Mortimer, J. T., “Electrical properties of implant encapsulation tissue,” Ann. Biomed. Eng. 22, 23–33 (1994).
[11] Gabriel, C., “Compilation of the Dielectric Properties of Body Tissues at RF and Microwave Frequencies,” Report N.AL/OE-TR- 1996-0037, Occupational and environmental health directorate, Radiofrequency Radiation Division, Brooks Air Force Base, (1996).
[12] Labiner, D. M., Ahern, G. L., “Vagus nerve stimulation therapy in depression and epilepsy: therapeutic parameter settings,” Acta Neurol Scand. 115(1), 23-33 (2007).
[13] McIntyre, C.C., Richardson, A.G., Grill, W.M., “Modeling the excitability of mammalian nerve fibers: influence of afterpotentials on the recovery cycle,” J Neurophysiol. 87(2), 995-1006 (2002).
[14] Rattay, F., “The basic mechanism for the electrical stimulation of the nervous system,” Neuroscience 89(2), 335-46 (1999).
[15] Hammer, N., Löffler, S., Cakmak, Y.O., et al., “Cervical vagus nerve morphometry and vascularity in the context of nerve stimulation - A cadaveric study,” Sci Rep. 8(1), 7997 (2018).